ISSN 2079-1372 Problems of Tribology, V. 31, No 2/120-2026, 44-51

Problems of Tribology
Website: http://tribology.khnu.km.ua/index.php/ProbTrib
E-mail: tribosenator@gmail.com

DOI: https://doi.org/10.31891/2079-1372-2026-120-2-44-51

Construction and application of the limit strain surface for evaluating the plasticity of porous bodies

R. Sivak[1] 0000-0002-7459-2585, **L. Polishchuk[1]** 0000-0002-5916-2413, **V. Shenfeld[1]*** 0000-0002-5548-6971, **A. Ormanbekova[2]** 0000-0001-8663-006X, **N. Zhumakhan[2]** 0000-0002-9548-6896

Vinnytsia National Technical University, Vinnytsia, Ukraine
Almaty Technological University, Almaty, Kazakhstan
**E-mail: leravntu@gmail.com*

Received: 10 April 2026: Revised 25 April 2026: Accept: 14 May 2026

Abstract

Traditional failure criteria for solid materials are not applicable to powder materials due to the presence of porosity, which acts as a sink for dislocations, alters defect accumulation kinetics, and slows structural degradation. This study presents a comprehensive analysis of the deformation behavior of cylindrical porous iron-based samples. The deformed state on the sample surface was determined using the coordinate grid method, while displacement measurements were performed with a high-precision instrumental microscope, enabling the calculation of strain rate components at each stage up to macrocrack formation. To ensure a wide variation of the stress state index and the Nadai–Lode parameter, eight loading paths were implemented, including free upsetting under different friction conditions and deformation in steel shells. The parameters η_0 and μ_σ were calculated considering porosity functions, ensuring an adequate representation of void effects on the stress state. Experimental data were processed using successive approximation methods to identify key model parameters. As a result, an analytical expression for the limit deformation surface was obtained, describing the failure condition of the material. A significant finding is the confirmation of the invariance of the plasticity resource of the base material with respect to initial porosity, provided the matrix composition and structure remain unchanged. This enables the obtained surface to be considered a universal characteristic of sintered iron. The developed approach provides a reliable tool for predicting defect formation and optimizing powder metallurgy processes such as pressing, calibration, and bulk forming.

Keywords: destruction, porosity, damage accumulation, stress-strain state, stress state index

Introduction

The importance of researching porous structures stems from their unique ability to combine low specific gravity with high functional capabilities. The development of accurate computational models for predicting the physico-mechanical properties of materials resulting from plastic processing critically depends on changes in porosity and becomes a primary task for ensuring the required technological heredity of products.

The transition to the analysis of 3D environments has allowed for the identification of the influence of cell shape and cross-sectional heterogeneity of struts on plasticity, emphasizing the insufficiency of simplified 2D approaches for an adequate description of micro-scale effects. An important step in this direction was the work [1], which proposed a methodology for generating 3D open-cell porous materials based on space partitioning into regions, where each region contains points closer to one center than to others. The authors demonstrated that the anisotropy of such structures is determined by the pore growth trajectory along the z-axis, while the randomness of pore size and their spatial distribution in the xy-plane creates a complex effect of weakening the mechanical properties.

These microstructural studies establish the foundation for transitioning from the analysis of individual structural elements to a phenomenological description at the macroscale. The development of macroscopic yield models has progressed from the criterion [2], which is based solely on the first and second stress invariants and is limited to circular deviatoric cross-sections, to more complex surfaces. An attempt to expand this framework was the flexible criterion [3] for granular media; however, it proved incapable of describing the change in the

orientation of the triangular cross-section along the hydrostatic axis. In the study [4], a modification of the Ehlers model was proposed, allowing for the correct orientation of the triangular deviatoric cross-sections of the yield surface depending on the sign of the hydrostatic pressure.

Despite significant progress, a substantial gap remains regarding the description of plastic behavior under large hydrostatic loading components and the inclusion of Lode angle dependence [5]. Existing models often ignore the influence of the third invariant of the stress deviator, which is critical for porous bodies where the shape of the yield surface transforms from tension to compression [6]. Neglecting these effects leads to significant errors in predicting the onset of plastic flow under conditions of complex triaxial stress states [7]. The lack of a holistic approach that combines the random nature of 3D microstructure with refined phenomenological criteria hinders the design of high-reliability products operating under critical loading regimes.

The aim of this study is to develop a methodology for constructing limit strain surfaces for porous bodies $\Gamma_{op}(\eta_0,\mu_\sigma)$ depending on the stress state index of the base material η_0 and the Nadai-Lode parameter μ_σ. This is based on experimental studies of the upsetting process of cylindrical specimens under various contact friction conditions and within shells, as well as obtaining the limit strain surface for an iron-based porous material, which will allow for the prediction of the technological heredity indicators of products.

Object and Methods of Research

During the plastic deformation of porous bodies, the damage accumulation process is more complex than during the same deformation of solid bodies, as in this case, plastic loosening occurs simultaneously with the material compaction process. The determining factor during fracture is not "loosening" in general (i.e., overall porosity), but the development and accumulation of micropores and microcracks within the skeleton material. Furthermore, pores act as sinks for dislocations, which slows down the rate of damage accumulation. In macroscopic experiments, it is impossible to separate the processes of material compaction and loosening. Therefore, to evaluate the plasticity of porous bodies, the strain accumulated in the base material at the moment of fracture was adopted as the measure of plasticity [8, 9].

$$\Gamma_{OP} = \int_0^{t_p} \dot{\gamma}_0 d\tau, \tag{1}$$

where t_p – is the deformation time until fracture;

$$\dot{\gamma}_0^2 = \frac{f_2(\theta)\dot{e}^2}{(1-\theta)} + \frac{f_1(\theta)\dot{\gamma}^2}{(1-\theta)};$$

$$\dot{\gamma} = \sqrt{\left(\dot{e}_{ij} - \frac{1}{3}\dot{e}\delta_{ij}\right)\left(\dot{e}_{ij} - \frac{1}{3}\dot{e}\delta_{ij}\right)},$$

$\dot{\gamma}$ is the intensity of the strain rate deviator;
$\dot{\gamma}_0\ is$ the intensity of the strain rate deviator in the base material;
$\dot{e}_{ij}$ is the components of the strain rate tensor;
$\dot{e} = \delta_{ij}\dot{e}_{ij}$ is the rate of relative volume change;
$f_1(\theta), f_2(\theta)$ are the porosity functions;
θ - porosity.
In general, the cold plastic limit strain of the base material depends on a number of factors:

$$\Gamma_{op} = f(x_i,c_j,\eta,\mu_\sigma,\theta), \tag{2}$$

where x_i is parameters that account for the influence of chemical composition and sintering conditions;
c_j is the influence of structure;
η, μ_σ are the influence of the stress state scheme.

Chemical composition and structure characterize the inherent plasticity of the material. The influence of the latter is established during experimental studies conducted according to specific programs. As a result, dependency (2) takes the following form:

$$\Gamma_{op} = f[\eta(\Gamma_o,\theta),\mu_\sigma(\Gamma_o,\theta)], \tag{3}$$

where Γ_o is the strain accumulated in the base material at a given moment in time.

Thus, during the cold plastic deformation of porous bodies, the primary factors determining plasticity are the stress state scheme and porosity. The dependence of plasticity on the stress state scheme is

described by the limit strain surface $\Gamma_{op}(\eta_0,\mu_\sigma)$. In this dependency, one of the arguments is the stress state index of the base material [8, 9].

$$\eta_0 = \eta \sqrt{\frac{f_1(\theta)}{(1-\theta)\left(\frac{1f_1(\theta)}{6f_2(\theta)}\eta^2+1\right)}}, \tag{4}$$

where $\eta = \frac{I_1(T_\sigma)}{\sqrt{J_2(D_\sigma)}} = \sqrt{6}\frac{p}{\tau}$ - the stress state index of a porous body;

$p = \frac{1}{3}\sigma_{ij}\delta_{ij}$ – average stress;

$\tau = \sqrt{(\sigma_{ij} - p\delta_{ij})(\sigma_{ij} - p\delta_{ij})}$ - the stress deviator intensity;

σ_{ij} - Components of the stress tensor.

To construct the limit strain surface $\Gamma_{op}(\eta_0,\mu_\sigma)$ for a porous body, it is necessary to ensure conditions where η_0 = const and μ_σ = const throughout the entire deformation process. During the plastic deformation of porous bodies, realizing such conditions is practically impossible. Therefore, to obtain the $\Gamma_{op}(\eta_0,\mu_\sigma)$ relationship, tests were conducted under loading conditions close to simple loading. In this case, the hypothesis of a linear damage accumulation law is valid [10, 11]. Thus, the fracture condition can be written as [8]:

$$\psi = \int_0^{\Gamma_{op}} \frac{d\Gamma_0}{\Gamma_{op}(\mu_\sigma,\eta_0)} = 1, \tag{5}$$

where ψ - used plasticity resource;

Γ_{op} - accumulated strain of the base material at the onset of a macrocrack.

$\Gamma_{op}(\eta_0,\mu_\sigma)$ - limit strain surface.

Based on the analysis of experimental results, the following relationship was adopted to approximate $\Gamma_{op}(\eta_0,\mu_\sigma)$

$$\Gamma_{op}(\eta_0,\mu_\sigma) = \Gamma_{op}(0,0)\exp(\lambda_2\mu_\sigma - \lambda_1\eta) \tag{6}$$

where $\lambda_1 = ln\left(\frac{\Gamma_{op}(-1,0)}{\Gamma_{op}(0,0)}\right)$, $\lambda_2 = ln\left(\frac{\Gamma_{op}(0,1)}{\Gamma_{op}(0,0)}\right)$, $\Gamma_{op}(0,0)$, $\Gamma_{op}(-1,0)$, $\Gamma_{op}(0,1)$ - Limit strains of the base material at η_0=0, μ_σ=0, η_0=-1, μ_σ=0, η_0=0, μ_σ=1 respectively.

The following methodology was used to construct the $\Gamma_{op}(\eta_0,\mu_\sigma)$ relationship. At the first stage, a plasticity diagram was constructed. During the construction of plasticity diagrams, a plane stress state occurs, where σ_2 = 0 i, and, as shown in [8], in this case η = -μ. Therefore, formula (6) is reduced to the form:

$$\Gamma_{op}(\eta_0,\mu_\sigma) = \Gamma_{op}(0,0)\exp(-\lambda\eta), \tag{7}$$

where $\lambda=\lambda_1+\lambda_2$. (8)

Problem Statement

Based on experimental studies of the upsetting process of cylindrical specimens under various contact friction conditions and within cladding, it is necessary to develop a methodology for constructing the limit strain surfaces $\Gamma_{op}(\eta_0,\mu_\sigma)$ for porous bodies and to obtain the limit strain surface for an iron-based porous material.

Results and Discussion

To determine the limit strain Γ_{op} for various deformation paths, free upsetting tests were conducted on cylindrical specimens made of iron-based porous material with three initial porosities: θ_0=0.27, θ_0=0.214, θ_0=0.128. The initial dimensions of the specimens were h=15.5 mm, d=11.3 mm. Upsetting was performed under various contact friction conditions, as well as with constrained (clamped) ends.

The strain state on the free surface of the specimens was determined using the grid method (coordinate-measuring grid method). For this purpose, marks were applied in the axial and tangential directions in the middle-height section of the specimen using a Vickers hardness tester, spaced circumferentially at 120^0. The initial distance between the marks was a_0=2mm. Initial and current values of a were measured using a toolmaker's microscope with an accuracy of 0.005 mm. To ensure identical deformation paths, determined by consistent friction conditions at the specimen-tool contact interface, 5 to 6 specimens were selected for each initial porosity. The variation in porosity within a batch did not exceed $\Delta\theta_0$ = 0.005. Each specimen was then upset in stages $\left(\frac{\Delta h_i}{h} = 0.05\ldots0.07\right)$ until a macrocrack with a length of 0.5...1.0 мм appeared. At each stage, the strain components e_z, e_φ were determined. The degree of strain at the moment of fracture was refined by upsetting a control specimen

until failure, which was conducted in 1...3 stages. After determining the limit strain, one specimen from the batch was upset to various degrees of reduction. From the resulting 5 to 6 upset specimens, a half-ring was cut from the "barrel" region, and its density was determined by hydrostatic weighing.

Since a model of a strain-hardening plastic porous body is being considered, real time can be excluded from the physical equations. Therefore, for the upsetting process, the parameter adopted as the time substitute (or time-like parameter) was [9].

$$t = 2\,ln\frac{D}{D_0}. \tag{9}$$

Taking into account the chosen parameter t, the strain rates and the volumetric strain rate were determined.

$$\dot{e} = \frac{\dot{\theta}}{1-\theta} \tag{10}$$

The intensity of the strain rate deviator was determined using the formula:

$$\dot{\gamma} = \sqrt{\left(\dot{e}_z - \frac{1}{3}\dot{e}\right)^2 + \left(\dot{e}_\phi - \frac{1}{3}\dot{e}\right)^2 + \left(e_r - \frac{1}{3}\dot{e}\right)^2}. \tag{11}$$

The accumulated intensity of the strain deviator was determined by numerical integration.

$$\Gamma = \int_0^t \dot{\gamma}\,d\tau. \tag{12}$$

The stress state index η was calculated using the formula:

$$\eta = -\sqrt{6}\frac{\dot{e}_r - \frac{1}{3}\dot{e}}{\dot{\gamma}}, \tag{13}$$

in the derivation of which it was taken into account that $\sigma_r = 0$ i on the free surface, and the flow theory relations [12] were utilized. The accumulated strain of the base material was calculated using the formula $\Gamma_0 = \int_0^t \dot{\gamma}_0 d\tau$, while the stress state index η_0 was determined by (4). During free upsetting under various contact friction conditions and upsetting with constrained ends, the relations $\sigma_\varphi = \sigma_1$, $\sigma_2 = 0$ and $\sigma_3 = \sigma_z$ hold in the equatorial region; therefore, the Nadai-Lode parameter is equal to:

$$\mu_\sigma = \frac{2\sigma_2 - \sigma_1 - \sigma_3}{\sigma_1 - \sigma_3} = \frac{2\dot{e}_r - \dot{e}_\phi - \dot{e}_z}{\dot{e}_\phi - \dot{e}_z}. \tag{14}$$

The deformation paths in the Γ_0 - η_0, μ_σ coordinates, obtained after processing the experimental data, are shown in Fig. 1.

It was hypothesized that the limit strain Γ_{op} during the cold plastic deformation of porous materials depends only on the base material and the parameters η_0 and μ_σ independent of the initial porosity θ_0.

The constants $\Gamma_{op}(0,0)$, λ of the porous sintered material, which depend on the powder particle size distribution, its chemical composition, pressing and sintering conditions, etc., are subject to experimental determination.

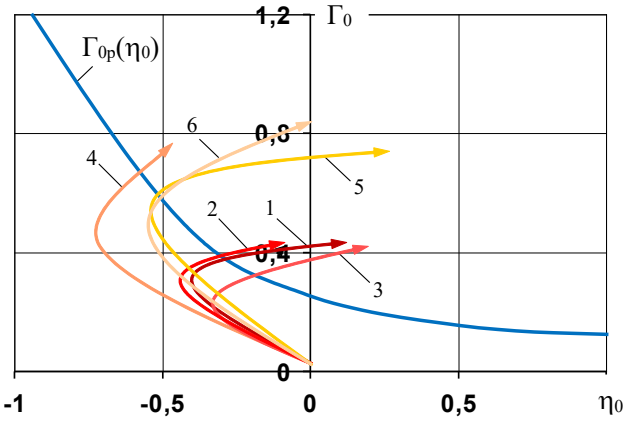

Fig. 1. Plasticity diagram and deformation paths in η_0-Γ_0 coordinates

Taking into account (7), the fracture criterion (5) takes the form:

$$\int_0^{\Gamma_{op}^*} exp(\lambda,\eta)\, d\Gamma_0 = \Gamma_{op}(0,0), \tag{15}$$

where Γ_{op}^* - the limit strain of the base material for a given deformation path.

Equations (15) were formulated for 8 deformation paths. By equating the left-hand sides of (15), four equations were obtained, from which the value λ=1.55 was determined using the method of successive approximations. Given the known value of λ, the value $\Gamma_{op}(0,0) = 0.28$ was found from (15).

Thus, for the dependence $\Gamma_{op}(\eta_0)$ under the condition $\eta = -\mu_\sigma$ the following was obtained:

$$\Gamma_{op}(\eta_0) = 0.28\exp(-1.55\eta_0). \tag{16}$$

The resulting plasticity diagram for the porous material, $\Gamma_{op}(\eta_0)$ is shown in Fig. 1, as well as in Fig. 2 as a curve obtained from the intersection of the plane $\eta_0 = -\mu_\sigma$ with the surface $\Gamma_{op}(\eta_0,\mu_\sigma)$.

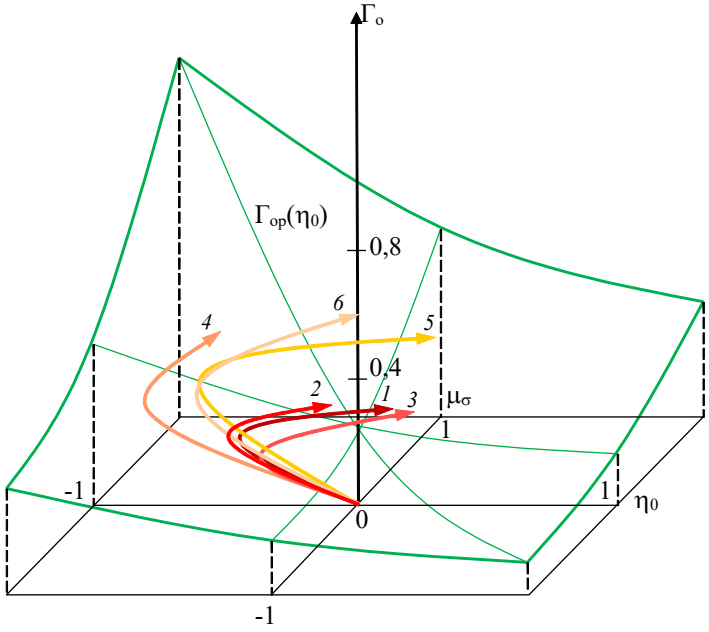

Fig. 2. Limit strain surface and deformation paths in η_0 - μ_σ - Γ_0 coordinates for a sintered iron-based porous material

To obtain other points on the limit strain surface $\Gamma_{op}(\eta_0,\mu_\sigma)$, cylindrical specimens with three initial porosities $\theta_0 = 0.27$, $\theta_0 = 0.214$, $\theta_0 = 0.128$ were upset in jackets. In doing so, it was assumed that the condition on the specimen surface is fulfilled:

$$\sigma_r = \sigma_{r0}, \tag{17}$$

where σ_{r0} - is the radial stress on the specimen surface and σ_r - is the radial stress on the inner surface of the jacket, which was determined according to the procedure [13]. Upsetting was performed in jackets with an inner diameter $d_{вн} = 8$ mm, $d_{н1} = 12$ mm, $d_{н2} = 16$ mm, $d_{н3} = 20$ mm.

The stress state index of the base material, η_0 in the critical zone (from a fracture perspective) was determined using formula (4). Meanwhile, the stress state index of the porous body, η , was determined by formula (18), which was derived using the relations of flow theory:

$$\eta = \sqrt{6}\frac{p}{\tau} = \sqrt{6}\left(\frac{\sigma_{r0}}{\tau} + \frac{\frac{1}{3}\dot{e} - \dot{e}_r}{\dot{\gamma}}\right). \tag{18}$$

In deriving (18), it was taken into account that

$$\frac{\dot{\gamma}}{\tau}p = \frac{\dot{\gamma}}{\tau}\sigma_{r0} - \dot{e}_r - \frac{1}{3}\dot{e}. \tag{19}$$

In the "barrel" region, it can be assumed that $\sigma_1 = \sigma_\varphi$, $\sigma_2 = \sigma_{r0}$, $\sigma_3 = \sigma_z$, then, the following formula for calculating the Lode parameter is obtained:

$$\mu_\sigma = \frac{2\sigma_{r0} - \sigma_\phi - \sigma_z}{\sigma_\phi - \sigma_z}. \tag{20}$$

The values of $\dot{e}_r$, $\dot{e}_\phi$, $\dot{e}_z$ were determined by the distortion of the dividing grid applied to the specimen surface. The stresses were found according to the procedure [13]. By analogy with (15) and taking into account (9), the fracture criterion (5) takes the form:

$$\int_0^{\Gamma_{op}^*} exp(-\lambda_2\mu_\sigma + (\lambda - \lambda_2)\eta)\, d\Gamma_0 = \Gamma_{op}(0,0). \tag{21}$$

Equations (21) were formulated for six deformation paths. By equating the left-hand sides of (21), three equations were obtained, from which the value λ_2=0.857 was determined using the method of successive approximations.

As a result, the following formula for the limit strain surface was obtained:

$$\Gamma_{op}(\eta_0, \mu_\sigma) = 0{,}28\, exp(-0.857\mu_\sigma - 0.69\eta_0) \tag{22}$$

in which λ_1 = 0,69. The resulting limit strain surface $\Gamma_{op}(\eta_0,\mu_\sigma)$ is shown in Fig. 2.

Conclusions

The processes of plastic deformation in porous bodies are determined by a complex combination of macroscopic densification and strain-induced loosening mechanisms. The significance of the study lies in establishing fundamental laws of fracture based on the analysis of damage accumulation directly within the material skeleton. The obtained results demonstrate alignment with the stated objectives, proving that the state of the base material is the decisive factor in the exhaustion of the plasticity resource. In the course of the study, it was substantiated and confirmed that the mathematical model of the limit strain surface fully validates the theoretical assumptions regarding the dependence of the limit state on the stress state index of the base material η_0 and the stress state type parameter μ_σ (Lode parameter). The results achieved provide a solid foundation for transitioning from empirical estimations to the analytical prediction of limit forming. The methodological integrity of the work is ensured by strict adherence to the sequential stages of experimental research and the precision of measurement procedures. The study is based on a comprehensive analysis of the deformation of sintered iron under various loading paths. The implementation of the research included the following stages: specimen preparation, deformation, measurement of the coordinates of the dividing grid nodes, and determination of the moment of fracture (macro-crack initiation). This methodological approach allowed for the transformation of primary experimental data into a verified physico-mathematical model. Consequently, the article proposes a methodology for constructing the limit strain surface of porous bodies in the following coordinates: the limit strain of the base material Γ_{op}, the stress state triaxiality (index) of the base material η_0, and the Lode parameter μ_σ. The methodology enables the derivation of the limit strain surface of a porous body $\Gamma_{op}(\eta_0,\mu_\sigma)$ based on compression tests of cylindrical specimens under various contact friction conditions and within jackets.

References

1. Chen, K., Qin, H. & Ren, Z. (2023). *Establishment of the microstructure of porous materials and its relationship with effective mechanical properties.* Sci Rep 13, 18064. https://doi.org/10.1038/s41598-023-43439-6

2. Zepeda-Ruiz, Luis A. and Stukowski, Alexander and Oppelstrup, Tomas and Bulatov, Vasily V. (2017). *Probing the limits of metal plasticity with molecular dynamics simulations.* Nature. Volume 550, number 7677, pages 492–495. https://doi.org/10.1038/nature23472

3. Yang, Yangyiwei and Bharech, Somnath and Finger, Nick and Zhou, Xiandong and Schröder, Jörg and Xu, Bai-Xiang. (2024). *Elasto-plastic residual stress analysis of selective laser sintered porous materials based on 3D-multilayer thermo-structural phase-field simulations*. npj Computational Materials. Volume 10, number 1. https://doi.org/10.1038/s41524-024-01296-5

4. Abendroth, Martin, Malik, Alexander, Kiefer, Björn. (2023). *A Modified Ehlers Model for the Description of Inelastic Behavior of Porous Structures.* Institut for Mechanics and Fluid Dynamics, TU Bergakademie Freiberg. https://doi.org/10.2139/ssrn.4651521

5. H. A. Bahliuk, S. F. Kyryliuk. (2023). Evoliutsiia protsesu ushchilnennia ta deformovanoho stanu poruvatykh zahotovok pry yikh hariachomu shtampuvanni u vidkrytomu shtampi. Mech. Adv. Technol. Vol. 7, No. 3, pp. 350–355. https://doi.org/10.20535/2521-1943.2023.7.3.292713

6. Patnaik, S., Jokar, M., Ding, W. et al. (2022) *On the role of the microstructure in the deformation of porous solids*. npj Comput Mater 8, 152. https://doi.org/10.1038/s41524-022-00840-5

7. Lindqwister, Winston, Peloquin, Jacob, Dalton, Laura, Gall, K. (2025). *Predicting compressive stress-strain behavior of elasto-plastic porous media via morphology-informed neural networks*. Communications Engineering. VL 4. https://doi.org/10.1038/s44172-025-00410-9

8. Sivak I. O. (1996). *The evaluation of deformability of the porous bodies*. The Bulletin of the Polytechnic Institute of Jassy. XLII (XLVI), № 3(4). P. 607– 611.

9. Ogorodnikov V. A., Derevenko I. A., Sivak R. I. (2018). *On the influence of curvature of the trajectories of deformation of a volume of the material by pressing on its plasticity under the conditions of complex loading*. Materials science. 54, № 3. P. 326–332. https://doi.org/10.1007/s11003-018-0188-x

10. O. V. Hrushko, V. A. Ohorodnikov, Yu. O. Slobodianiuk. (2019). Deformovnist malovuhletsevoho drotu v protsesi yoho bahatostupinchastoho kholodnoho volochinnia, Visnyk Vinnytskoho politekhnichnoho instytutu, № 3, S. 103-110. https://doi.org/10.31649/1997-9266-2019-144-3-103-110

11. Mirzaei, A. M., Mirzaei, A. H., Sapora, A. et al. (2025). *Strain based finite fracture mechanics for fatigue life prediction of additively manufactured samples*. Int J Fract 249, 44. https://doi.org/10.1007/s10704-025-00855-1

12. Shtern, M.B., Mikhailov, O.V. (2003). *Numerical Modelling of the Compaction of Powder Articles of Complex Shape in Rigid Dies: Effect of Compaction Scheme on Density Distribution. Part 2. Modelling Procedure and Analysis of Forming Schemes*. Powder Metall. Met. Ceram. 42, 114–121. https://doi.org/10.1023/A:1022928118809

13. Laptiev, A. V. (2024). *New Die-Compaction Equations for Powders as a Result of Known Equations Correction: Part 1–Review and Analysis of Various Die-Compaction Equations*. Powders, 3(1), 111-135. https://doi.org/10.3390/powders3010008

14. Bernard-Granger, Guillaume and Benameur, Nassira and Addad, Ahmed and Nygren, Mats and Guizard, Christian and Deville, Sylvain. (2009). *Phenomenological analysis of densification mechanism during spark plasma sintering of MgAl2O4*. Journal of Materials Research. Volume 24, number 6. Pages 2011–2020. https://doi.org/10.1557/jmr.2009.0243

15. Manière, Charles and Olevsky, Eugene A. (2017). *Porosity dependence of powder compaction constitutive parameters: Determination based on spark plasma sintering tests*. Scripta Materialia. Volume 141. Pages 62–66. https://doi.org/10.1016/j.scriptamat.2017.07.026

16. Al-Qureshi, H.A.; Soares, M.R.F.; Hotza, D.; Alves, M.C.; Klein, A.N. (2008). *Analyses of the fundamental parameters of cold die compaction of powder metallurgy*. J. Mater. Process. Technol. 199, 417–424. https://doi.org/10.1016/j.jmatprotec.2007.08.030

17. Aryanpour, G.; Farzaneh, M. (2015). *Application of a piston equation to describe die compaction of powders*. Powder Technol. 277, 120–125. https://doi.org/10.1016/j.powtec.2015.02.032

18. Molinari, A., Cristofolini, I., Pederzini, G., Rambelli, A. (2018). *A densification equation derived from the stress-deformation analysis of uniaxial cold compaction of metal powder mixes*. Powder Metall. 61, 210–218. https://doi.org/10.1080/00325899.2018.1466501

19. Haim Kalman. (2020). *Phenomenological study of particulate materials compression – From individual through bed compression to tableting*. Powder Technology. Volume 372, pages 161-177. https://doi.org/10.1016/j.powtec.2020.05.115

20. Montes, J.M.; Cuevas, F.G.; Cintas, J.; Ternero, F.; Caballero, E.S. (2018). *On the compressibility of metal powders*. Powder Metall. 61, 219–230. https://doi.org/10.1080/00325899.2018.1467074

Сивак Р.І., Поліщук Л.К., Шенфельд В.Й., Орманбекова А.А., Жумакхан Н. Побудова та застосування поверхні граничних деформацій для оцінки пластичності пористих тіл

Традиційні критерії руйнування суцільних матеріалів є непридатними для порошкових систем через наявність пористості, яка виступає стоком для дислокацій, змінює кінетику накопичення дефектів і уповільнює процеси структурної деградації. У роботі виконано комплексний аналіз деформування циліндричних зразків пористого матеріалу на основі заліза. Деформований стан на поверхні визначали методом координатних сіток, а переміщення міток вимірювали за допомогою високоточного інструментального мікроскопа, що дозволило розрахувати компоненти швидкостей деформацій на всіх стадіях навантаження до утворення макротріщин. Для охоплення широкого діапазону індексу напруженого стану та параметра Надаї–Лоде реалізовано вісім траєкторій навантаження, включаючи вільне осадження за різних умов тертя та деформування в сталевих оболонках. Розрахунок параметрів η_0 та $\mu\sigma$ виконано з урахуванням функцій пористості, що забезпечило коректне врахування впливу пор на напружений стан матеріалу. Експериментальні дані узагальнено методом послідовних наближень, що дозволило визначити ключові параметри моделі. У результаті отримано аналітичну залежність поверхні граничних деформацій, яка описує умову руйнування матеріалу. Підтверджено інваріантність ресурсу пластичності базового матеріалу відносно початкової пористості за умови незмінності складу та структури матриці. Практична цінність полягає у створенні інструменту прогнозування дефектоутворення та оптимізації процесів порошкової металургії.

Ключові слова: руйнування, пористість, накопичення пошкоджень, напружено-деформований стан, показник напруженого стану